Optics Letters

Broadband supercontinuum generation in all-normal dispersion chalcogenide microwires

Alaa Al-Kadry,[1,*] Lizhu Li,[1] Mohammed El Amraoui,[2] Thibault North,[1] Younès Messaddeq,[2] and Martin Rochette[1]

[1]Department of Electrical and Computer Engineering 3480 University Street, McGill University, Montréal (Québec), H3A 0E9, Canada
[2]COPL, 2375 rue de la Terrasse, Laval University, Québec (Québec) G1 V 0A6, Canada
*Corresponding author: alaa.al-kadry@mail.mcgill.ca

Received 19 August 2015; revised 9 September 2015; accepted 13 September 2015; posted 18 September 2015 (Doc. ID 248215); published 9 October 2015

We report the first chalcogenide microwire designed with all-normal dispersion to generate supercontinuum by optical wave breaking, a low-noise nonlinear process. The chalcogenide (As_2S_3) microwire is coated with PMMA and tapered to a diameter of 0.58 μm to achieve the all-normal dispersion regime. The generated supercontinuum spectrum spans over an octave from 960 to >2500 nm using a microwire length of only 3 mm and a low pulse energy of 150 pJ.

OCIS codes: (060.2310) Fiber optics; (060.2280) Fiber design and fabrication; (060.4370) Nonlinear optics, fibers.

http://dx.doi.org/10.1364/OL.40.004687

Broadband supercontinuum (SC) sources are important for applications such as frequency metrology [1], optical coherence tomography [2], and ultrashort pulse compression [3]. Microwires and photonic crystal fibers receive much attention for broadband SC generation because of the ability to engineer their dispersion and nonlinear properties [4,5]. These fibers are usually designed to produce maximum spectral bandwidth such that the pump wavelength is close to the fiber's zero-dispersion wavelength (ZDW) and lies in the anomalous dispersion range [6–8]. For this type of SC, the spectral broadening mainly results from soliton fission, which is sensitive to shot-to-shot fluctuations, and modulation instability, which is seeded from noise [9]. Both nonlinear processes lead to phase noise and unstable amplitude across the spectrum [10]. However, this noise can be reduced through suppressing soliton fission by engineering the fiber group-velocity dispersion (GVD) so that it is normal over the SC bandwidth [11].

A wide range of normally dispersive silica fibers has been designed for SC generation. This includes, for example, dispersion shifted fibers [12], photonic crystal fibers [13–15], microwires [16], and highly nonlinear fibers [17]. In silica microwires designed with normal dispersion, an octave SC was demonstrated in the ultraviolet wavelength range [16]. A pump source was chosen at a wavelength of 400 nm in order to experience a low magnitude of normal dispersion.

Chalcogenide (ChG) fibers, which exhibit a large value of normal dispersion, have also been investigated for SC generation [18–21]. These fibers are excellent candidates for broadband SC generation because of their high nonlinearity and their wide transparency [22]. A SC is generated in the normal dispersion by pumping far below the ZDW, so that the generated spectrum does not extend into the anomalous dispersion regime. However, the large normal dispersion value at the available commercial laser wavelengths increases the power requirements for broadband SC generation [20,23]. A more efficient method, and the one used in this study, is to generate SC in a ChG microwire with an all-normal GVD profile and a low value of dispersion at the pump wavelength.

In this Letter, we present the first ChG microwire designed with all-normal dispersion to generate SC by optical wave breaking, a low-noise nonlinear process. The microwire structure of As_2S_3 core with PMMA cladding and tapering to a diameter of 0.58 μm are essential in the achievement of always normal GVD. In addition to providing the microwire an all-normal GVD, the PMMA cladding also improves the microwire mechanical strength [24]. The large nonlinearity, the reduced chromatic dispersion from PMMA cladding, and the low absorption loss of the microwire lead to the generation of a SC with more than an octave of bandwidth from 960 to >2500 nm using a microwire length of only 3 mm and a low pulse energy of 150 pJ.

The efficiency of SC generation in the anomalous dispersion regime can be measured by the dimensionless parameter N, known as the soliton number, given as [25]

$$N = \sqrt{\frac{L_D}{L_{NL}}} = \sqrt{\frac{\gamma}{|\beta_2|}}\sqrt{\frac{ET}{2}}, \tag{1}$$

where L_D is the dispersion length, L_{NL} is the nonlinear length, γ is the waveguide nonlinearity, β_2 is the GVD, E is the pulse energy, and T is the pulse duration. Although soliton propagation is inhibited in the normal dispersion regime, N remains a useful parameter to measure the efficiency of SC generation by optical wave breaking [25]. Equation (1) indicates that for a

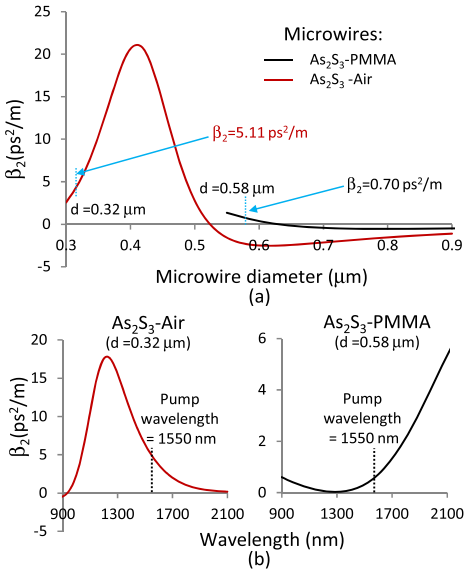

Fig. 1. (a) Chromatic dispersion profiles of As_2S_3-Air and As_2S_3-PMMA microwires as a function of diameter, at 1550 nm wavelength. (b) Chromatic dispersion profiles of As_2S_3-Air microwire with a diameter of 0.32 µm (red-line) and As_2S_3-PMMA microwire with a diameter of 0.58 µm (black-line).

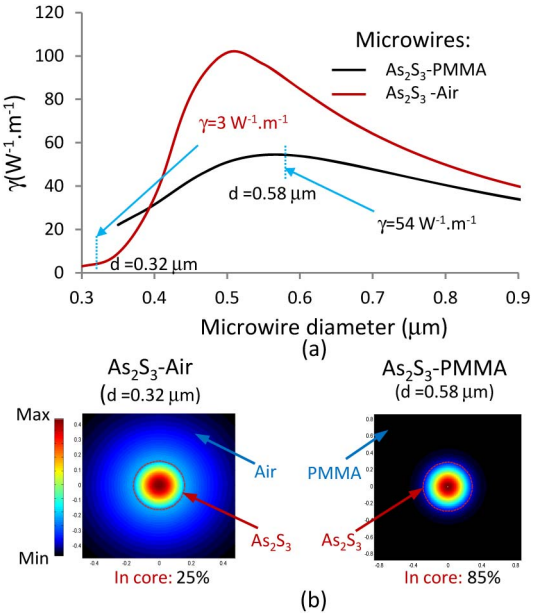

Fig. 2. (a) Waveguide-nonlinearity profiles of As_2S_3-Air and As_2S_3-PMMA microwires as a function of diameter, at 1550 nm wavelength. (b) Mode-field distribution of As_2S_3-Air microwire with a diameter of 0.32 µm and As_2S_3-PMMA microwire with a diameter of 0.58 µm.

given pulse with defined pulse energy and duration, the magnitude of N depends on fiber parameters γ and β_2. Therefore, in order to get a large value of N, i.e., broadband SC generation, the value of γ must be large and β_2 must be small.

Figures 1(a) and 2(a) depict the values of GVD (β_2) and waveguide nonlinearity (γ) of As_2S_3 microwires surrounded by air (red-line) or by PMMA cladding (black-line) at a wavelength of 1550 nm. β_2 and γ are determined by solving the characteristic equation of an infinite cladding cylindrical waveguide to obtain the propagation constant β, the electric field distribution $\vec{E}$, and the magnetic field distribution $\vec{H}$ for the fundamental mode [26]. Solving the characteristic equation takes into account the wavelength dependence of the refractive index of As_2S_3 obtained from the Sellmeier formula given in [27] and the refractive index of PMMA from the Cauchy relation given in [28]. The waveguide nonlinearity is calculated following the procedure of [29] with a nonlinear refractive index $n_2 = 5.44 \times 10^{-18}$ m^2/W [30] at 1550 nm wavelength. Figure 1(a) reveals that As_2S_3-Air microwires have to be tapered to smaller diameters than As_2S_3-PMMA microwires to have normal GVD at a wavelength of 1550 nm. As_2S_3-Air microwires with diameters smaller than 0.52 µm exhibit two ZDWs located at wavelengths shorter than 1550 nm. At a diameter of 0.32 µm, As_2S_3-Air microwires have a GVD profile (red-line) that is normal between 940 and 2100 nm wavelengths, as shown in Fig. 1(b). For this diameter, the two ZDWs are located at 765 and 939 nm. The figure shows also that As_2S_3-PMMA microwires have a GVD profile that is normal at all wavelengths for a diameter value of 0.58 µm. The magnitude of β_2 at 1550 nm wavelength for As_2S_3-Air and As_2S_3-PMMA microwires is 5.11 ps^2/m and 0.70 ps^2/m, respectively. For the same diameter values, Fig. 2(a) shows that γ of As_2S_3-Air and As_2S_3-PMMA microwires is 3 W$^{-1}\cdot$m^{-1} and 54 W$^{-1}\cdot$m^{-1}, respectively. The waveguide nonlinearity of As_2S_3-Air microwires is smaller than that of As_2S_3-PMMA microwires at the selected diameters since the mode is less confined in the core of As_2S_3-Air microwires, as shown in Fig. 2(b). By substituting the values of γ and β_2 in Eq. (1), $N_{As_2S_3\text{-PMMA}}$ is ~12 times that of $N_{As_2S_3\text{-Air}}$. Therefore, the PMMA cladding leads not only to achieving all-normal dispersion but also lowers the power consumption for SC generation.

The experimental setup for the generation of SC is shown in Fig. 3(a). Pump pulses are launched from a mode-locked Er-doped fiber laser. The pulses have a FWHM duration of 590 fs at a repetition rate of 20 MHz. The central wavelength and the average power of the laser are 1550 nm and 3.8 mW, respectively. A variable optical attenuator is inserted to control the pulse energy delivered to the tapered fiber. Two optical spectrum analyzers (OSA) with two different detection ranges are used to measure the generated SC spectra from the tapered fiber. The detection ranges of the two OSAs are bounded by the spectral ranges from 0.6–1.7 µm and 1.2–2.5 µm.

Figures 3(b) and 3(c) show respectively an input facet of the hybrid fiber and a schematic of the tapered fiber used in

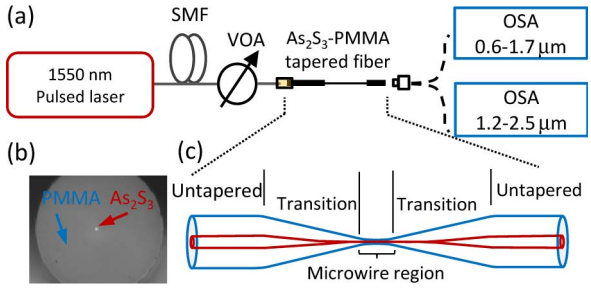

Fig. 3. (a) Experimental setup for SC generation. OSA: optical spectrum analyzer, VOA: variable optical attenuator. (b) Input facet of the hybrid fiber. (c) Schematic of the tapered fiber.

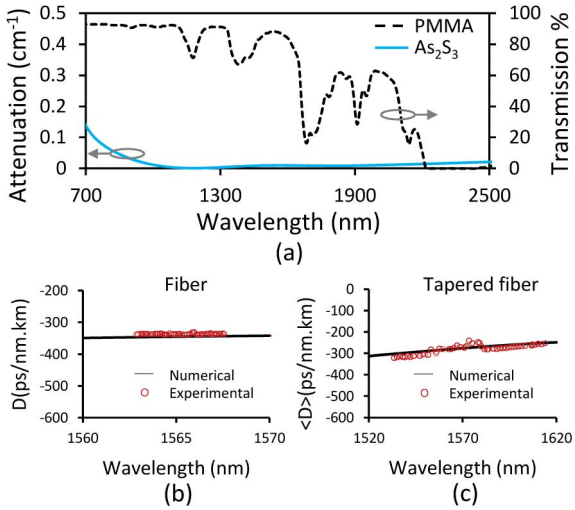

Fig. 4. (a) Absorption and transmission spectra of As_2S_3 and PMMA, respectively. Experimental and numerical calculations of D for As_2S_3-PMMA (b) fiber of 12 cm long, and (c) tapered fiber of 19.4 cm long with a microwire of 0.58 μm diameter.

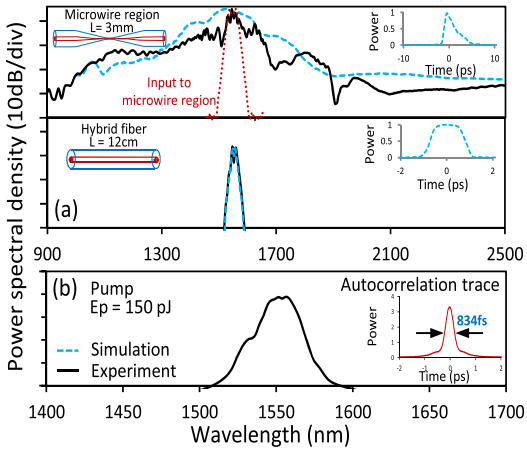

Fig. 5. (a) Experimentally generated (solid) and calculated (dashed) SC spectra from a hybrid fiber and a tapered fiber using pump energy of 150 pJ. Calculated input spectrum (dotted) to microwire region. The inset shows the temporal pulse profile from the hybrid fiber and the tapered fiber. (b) Pump spectrum together with the autocorrelation trace.

the experiment. The hybrid fiber is made of an As_2S_3 core surrounded by PMMA cladding, and its central part is tapered down adiabatically into a 3 mm long microwire using a tapering process described in [31]. The core size in the untapered region is 14 μm and is reduced down to 0.58 μm in the microwire region. The outer diameter of the PMMA is 500 μm in the untapered region and is reduced in the microwire region to 21 μm. One end of the hybrid fiber is butt-coupled to an SMF-28, and the fibers are bonded permanently with UV epoxy. The measured total insertion loss of the tapered fiber is 3.7 dB including Fresnel reflection losses, mode-mismatch at the hybrid fiber-SMF interfaces, microwire surface roughness losses [32], and misalignment at the SMF-As_2S_3 interfaces. Figure 4(a) shows the measured transmission spectrum of a 3 mm thick PMMA sheet (dashed-line) [33] and material loss of As_2S_3 glass (solid-line) [34]. Figures 4(b) and 4(c) show the calculated and experimental measurements of the dispersion parameter (D) for a 12 cm As_2S_3-PMMA fiber and the average value $\langle D \rangle$ for a 19.4 cm tapered fiber with a 3 mm microwire of 0.58 μm diameter, respectively. The figures show a good agreement between numerical calculation and experimental measurements of D.

Figure 5(a) depicts the experimentally generated (solid) SC spectra from a tapered fiber with a 3 mm long microwire of 0.58 μm diameter and a hybrid fiber 12 cm long using pump energy of 150 pJ. The generated SC spectrum from the tapered fiber covers a spectral bandwidth from 960 to >2500 nm at 35 dB below the peak value with the long wavelength edge being limited by the OSA. However, the spectral broadening of the pump pulse from the hybrid fiber is relatively small. This is because the pump experiences a large normal dispersion through the fiber. The value of N at the pump wavelength for a hybrid fiber is 3.2. Figure 5(b) depicts the pump spectrum together with the measured autocorrelation trace. The 834 fs autocorrelation duration corresponds to a pulsewidth of 590 fs.

To confirm the experimental results, numerical simulations of SC generation are also performed by solving the generalized nonlinear Schrödinger equation, using the Runge-Kutta interaction picture method. Figure 5(a) shows also the numerically calculated (dashed) SC spectra and temporal pulses profile from the hybrid fiber and the whole structure of the tapered fiber. The numerical simulations and the experimentally measured SC spectra agree reasonably well. The top plot in the figure shows also the numerically calculated (dotted) spectrum before entering the microwire region. The numerical calculations reveal that no significant spectral broadening occur in the untapered and down-taper transition region and the dominant SC broadening occurs in the microwire region. This is due to the long pulse duration and low pulse energy used to generate the SC [13,16]. The conservation of a single pulse in the time domain along the hybrid fiber and the tapered fiber indicates that SC broadening occurs in the normal dispersion regime [13]. These pulses are suitable for time-resolved applications and pulse compression. In the numerical simulation, a 590 fs sech pulse profile is assumed to propagate a path 224 cm along an SMF before the hybrid fiber or the tapered fiber. The pulse is discretized into 2^{14} samples with a temporal window width of 64 ps. The higher-order dispersion terms are included up to the 9th order. The contribution of self steepening and the delayed Raman response are also included with $f_R = 0.031$, $\tau_1 = 15.2$ fs and $\tau_2 = 230.5$ fs. The losses (i.e., intrinsic $\alpha(\lambda)$, coupling, and fabrication losses), and effective mode area $A_{\text{eff}}(\lambda)$ curves are used for the simulation.

Figure 6 depicts the experimentally generated SC spectra from a tapered fiber with a 0.58 μm microwire diameter as a function of the pulse energy. The pulse energy values presented in the figure take into consideration the coupling loss to the tapered fiber and correspond to N that increases from ~14 to 47. The dips in the spectra at 1678 and 1905 nm are attributed to PMMA absorption shown in Fig. 4.

In conclusion, we have introduced the first ChG microwire designed with all-normal dispersion to generate SC by optical wave breaking, a low-noise nonlinear process. The microwire structure of As_2S_3 core with PMMA cladding and tapering

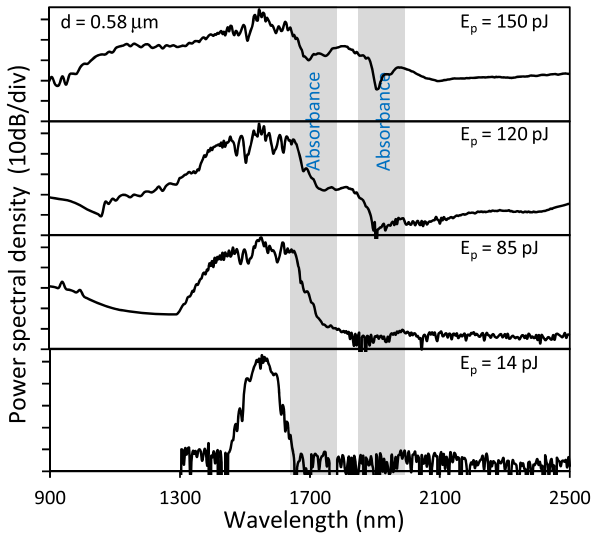

Fig. 6. Experimentally generated SC spectra using a 3 mm microwire with a diameter of 0.58 µm and for various pulse energy levels.

to an As_2S_3 diameter of 0.58 µm are essential in the achievement of the all-normal GVD. The tapering of the ChG hybrid fiber to a microwire of only 3 mm long generated a SC that covers more than an octave of bandwidth from 960 to >2500 nm using a low pulse energy of 150 pJ.

Funding. Fonds de Recherche Québecois Nature et Technologies (FRQNT) (173906).

REFERENCES

1. T. Udem, R. Holzwarth, and T. W. Hänsch, Nature **416**, 233 (2002).
2. I. Hartl, X. D. Li, C. Chudoba, R. K. Ghanta, T. H. Ko, J. G. Fujimoto, J. K. Ranka, and R. S. Windeler, Opt. Lett. **26**, 608 (2001).
3. Y. Liu, H. Tu, and S. A. Boppart, Opt. Lett. **37**, 2172 (2012).
4. T. Birks, W. Wadsworth, and P. Russell, Opt. Lett. **25**, 1415 (2000).
5. J. C. Knight, Nature **424**, 847 (2003).
6. J. Teipel, K. Franke, D. Turke, F. Warken, D. Meiser, M. Leuschner, and H. Giessen, Appl. Phys. B **77**, 245 (2003).
7. J. M. Dudley, G. Gënty, and S. Coen, Rev. Mod. Phys. **78**, 1135 (2006).
8. D. D. Hudson, S. A. Dekker, E. C. Mägi, A. C. Judge, S. D. Jackson, E. Li, J. S. Sanghera, L. B. Shaw, I. D. Aggarwal, and B. J. Eggleton, Opt. Lett. **36**, 1122 (2011).
9. G. Gënty, S. Coen, and J. M. Dudley, J. Opt. Soc. Am. B **24**, 1771 (2007).
10. K. L. Corwin, N. R. Newbury, J. M. Dudley, S. Coen, S. A. Diddams, K. Weber, and R. S. Windeler, Phys. Rev. Lett. **90**, 113904 (2003).
11. C. M. Netti, M. E. Zoorob, S. Roberts, M. D. Charlton, G. J. Parker, J. J. Baumberg, J. R. Lincoln, M. J. Lederer, and D. Kopf, Proc. SPIE **5690**, 222 (2005).
12. Y. Takushima and K. Kikuchi, IEEE Photon. Technol. Lett. **11**, 322 (1999).
13. A. Hartung, A. M. Heidt, and H. Bartelt, Opt. Express **19**, 12275 (2011).
14. I. A. Sukhoivanov, S. O. Iakushev, O. V. Shulika, J. A. Andrade-Lucio, A. Díez, and M. Andrés, Opt. Express **22**, 30234 (2014).
15. A. M. Heidt, A. Hartung, G. W. Bosman, P. Krok, E. G. Rohwer, H. Schwoerer, and H. Bartelt, Opt. Express **19**, 3775 (2011).
16. A. Hartung, A. M. Heidt, and H. Bartelt, Opt. Express **20**, 13777 (2012).
17. N. Nishizawa and J. Takayanagi, J. Opt. Soc. Am. B **24**, 1786 (2007).
18. L. Fu, V. G. Ta'eed, E. C. Mägi, I. C. M. Littler, M. Pelusi, M. R. E. Lamont, A. Fuerbach, H. C. Nguyen, D. I. Yeom, and B. J. Eggleton, Opt. Quantum Electron. **39**, 1115 (2007).
19. D. D. Hudson, M. Baudisch, D. Werdehausen, B. J. Eggleton, and J. Biegert, Opt. Lett. **39**, 5752 (2014).
20. R. R. Gattass, L. B. Shaw, V. Q. Nguyen, P. C. Pureza, I. D. Aggarwal, and J. S. Sanghera, Opt. Fiber Technol. **18**, 345 (2012).
21. C. R. Petersen, U. Møller, I. Kubat, B. Zhou, S. Dupont, J. Ramsay, T. Benson, S. Sujecki, N. Abdel-Moneim, Z. Tang, D. Furniss, A. Seddon, and O. Bang, Nat. Photonics **8**, 830 (2014).
22. J. L. Adam and X. Zhang, *Chalcogenide Glasses: Preparation, Properties and Applications*, 1st ed. (Woodhead Publishing, 2013).
23. J. M. Dudley and J. R. Taylor, *Supercontinuum Generation in Optical Fibers* (Cambridge University, 2010).
24. C. Baker and M. Rochette, Opt. Express **18**, 12391 (2010).
25. A. Hasegawa and F. Tappert, Appl. Phys. Lett. **23**, 142 (1973).
26. A. W. Snyder and J. D. Love, *Optical Waveguide Theory* (Chapman-Hall, 1983).
27. W. S. Rodney, I. H. Malitson, and T. A. King, J. Opt. Soc. Am. **48**, 633 (1958).
28. S. N. Kasarova, N. G. Sultanova, C. D. Ivanov, and I. D. Nikolov, Opt. Mater. **29**, 1481 (2007).
29. S. Afshar Vahid and T. M. Monro, Opt. Express **17**, 2298 (2009).
30. J. M. Harbold, F. Ö. Ilday, F. W. Wise, J. S. Sanghera, V. Q. Nguyen, L. B. Shaw, and I. D. Aggarwal, Opt. Lett. **27**, 119 (2002).
31. C. Baker and M. Rochette, IEEE Photon. J. **4**, 960 (2012).
32. G. Zhai and L. Tong, Opt. Express **15**, 13805 (2007).
33. I. Jones and J. Rudlin, *Joining Plastics* (National Physical Laboratory, 2006), pp. 25–26.
34. AMTIR-6: Arsenic Sulfide Glass As-S (2009). [Online]. Available: http://www.amorphousmaterials.com/products.